Crystallography

15C/ 2006G041

Observation of Interference Fringes Induced by Lattice Distortion in Resonant Scattering X-ray Topography II

Riichirou NEGISHI[*1], Tomoe FUKAMACHI[1], Masami YOSHIZAWA[1], Kenji HIRANO[1], Toshiyuki TANAKA[1], Tsuyoshi OBA[1],Keiichi, HIRANO[2], Takaaki KAWAMURA[3]
[1]Saitama Institute of Technology, 1690 Fusaiji, Fukaya, Saitama 369-0293, Japan
[2]Institute of Material Structure Science, KEK-PF, Oho, Tukuba, Ibaraki 305-0801, Japan
[3] University of Yamanashi, 4-4-37 Takeda, Kofu, Yamanashi 400-8510, Japan

We previously reported on topographs in which interference fringes by lattice distortion were observed when the Fourier coefficient of the imaginary part of X-ray polarizability χ_{hi} was zero for GaAs 200 reflection [1]. In this paper, we report on the contrast variation of the fringe for GaAs 200 reflection by changing the Bragg angle or the X-ray energy.

The experiment was carried out at BL-15C in KEK-PF. The X-rays from synchrotron radiation were monochromated by a Si 111 double-crystal and a GaAs 200 monochromator. The resultant topographic images are shown in Figs.1 and 2. Fig.1 shows an image recorded on the nuclear plate when X-ray energy is 9eV below the Ga K-absorption edge (10368eV) satisfying the condition $\chi_{hi} = 0$. Figs.2 (a) and (b) show the images when X-ray energy is 4eV and 1eV below the Ga K-absorption edge, respectively. The darker contrast corresponds to the higher X-ray intensity. The reciprocal lattice vector $\boldsymbol{h}$ is in the upward direction. Figs. 1(a) and (b) are the images for negative and positive $\Delta\theta$, respectively, where $\Delta\theta$ is the deviation angle from the Bragg condition. Figs. 2(a) and (b) are the images for negative$\Delta\theta$. The defect images A and B are observed in Figs.1 and 2(a), but the defect A is not visible in Fig.2 (b).

The interference fringes are observed clearly in Fig.1 (a) when $\Delta\theta$ is negative. The interference fringe α is observed in the dark band area, and the fringe spacing increases as the distance from A increases. The interference fringe β overlaps with the lower left of the defect B, and the fringe spacing increases as the distance from B increases. In Fig.1 (b), a dark band region is observed around the defect A. In the dark region, the interference fringe α' is observed in the opposite side of α, but no fringe is observed in the opposite side of α or β in Fig.1 (a). The fringe spacing of α'also increases as the distance from the defect A increases. The interference fringes α and β are also observed in Fig.2 (a), although the contrasts are weaker than those in Fig.1 (a). In Fig. 2(b), such fringes are scarcely observed. The contrast of the interference fringe becomes weak when $|\chi_{hi}|$ increases from zero as the X-ray energy becomes closer to the absorption edge from 9eV below it.

As shown in Fig. 1, the interference fringes are clearly observed in the peculiar condition $\chi_{hi} = 0$. The fringe area is restricted only in one side of each defect when $\Delta\theta$ is changed and the fringe spacing increases as the distance from the defect increases, which implies that the fringes are induced by the lattice distortion around the defect. Thus, it is noted that the interference fringes at $\chi_{hi} = 0$ are quite useful for elucidating lattice distortion structures.

[1] R. Negishi et al., KEK Progress Report, #**22**, 233(2005).

*negishi@sit.ac.jp

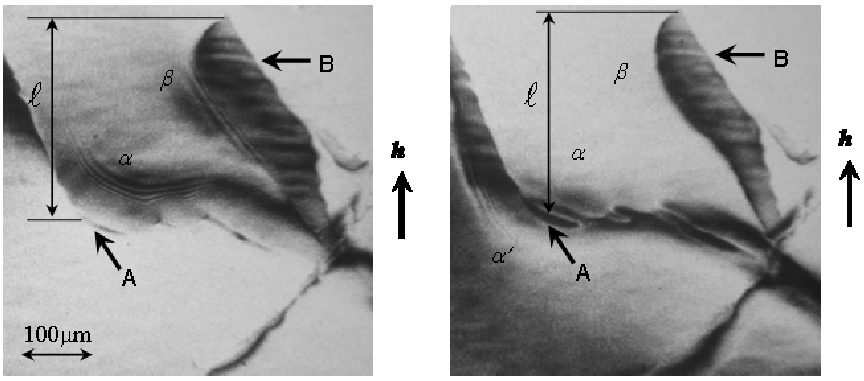

(a) Image at $-\Delta\theta$ (b) Image at $+\Delta\theta$

Fig.1 The topographs for GaAs 200 reflection at X-ray energy equal 10359eV($\omega_K - 9$eV).

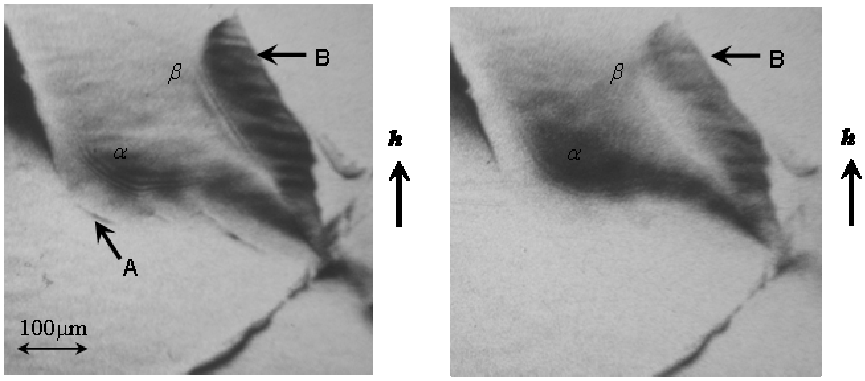

(a) Image at 10364eV ($\omega_K - 4$eV). (b) Image at 10367eV ($\omega_K - 1$eV).

Fig.2 The topographs at the differential energy of an X-ray.